This is a repository copy of *Thermotropic "plumber's nightmare" - a tight liquid organic double framework*.

White Rose Research Online URL for this paper:
https://eprints.whiterose.ac.uk/217714/

Version: Published Version

GDCh

Communication

Angewandte
Chemie
International Edition
www.angewandte.org

Liquid Crystals **Hot Paper**

Thermotropic "Plumber's Nightmare"—A Tight Liquid Organic Double Framework

Ya-Xin Li, Ruo-Yin Jia, Goran Ungar,* Tao Ma, Kai Zhao, Xiang-Bing Zeng,* and
Xiao-Hong Cheng*

Abstract: Gyroid, double diamond and the body-centred "Plumber's nightmare" are the three most common bicontinuous cubic phases in lyotropic liquid crystals and block copolymers. While the first two are also present in solvent-free thermotropics, the latter had never been found. Containing six-fold junctions, it was unlikely to form in the more common phases with rod-like cores normal to the network columns, where a maximum of four branches can join at a junction. The solution has therefore been sought in side-branched mesogens that lie in axial bundles joined at their ends by flexible "hinges". But for the tightly packed double framework, geometric models predicted that the side-chains should be very short. The true Plumber's nightmare reported here, using fluorescent dithienofluorenone rod-like mesogen, has been achieved with, indeed, no side chains at all, but with 6 flexible end-chains. Such molecules normally form columnar phases, but the key to converting a complex helical column–forming mesogen into a framework-forming one was the addition of just one methyl group to each pendant chain. A geometry-based explanation is given.

[*] Dr. Y.-X. Li, R.-Y. Jia
School of Chemistry and Chemical Engineering, Henan University of Technology, Zhengzhou 450001, China

Prof. G. Ungar
State Key Laboratory for Mechanical Behaviour of Materials, Shaanxi International Research Center for Soft Matter, Xi'an Jiaotong University, Xi'an 710049, China
E-mail: g.ungar@xjtu.edu.cn

T. Ma, K. Zhao, X.-H. Cheng
Key Laboratory of Medicinal Chemistry from Natural Resources, Ministry of Education, Yunnan University, 650091 Kunming, P. R. China
E-mail: xhcheng@ynu.edu.cn

Prof. G. Ungar, Dr. X.-B. Zeng
Department of Materials Science and Engineering, University of Sheffield, Sheffield S1 3JD, UK
E-mail: x.zeng@sheffield.ac.uk
    g.ungar@sheffield.ac.uk

Bicontinuous mesophases (BMs) are, beside Frank–Kasper phases,[1] the most intriguing self-assembled nanostructures in soft and hybrid matter. They provide a solution to a real mismatch between two subphases (e.g. oil-water, or aromatic-aliphatic) at their interface when that mismatch is moderate; a lesser mismatch is tolerated by smectic (lamellar) structures, while a larger mismatch is solved by columnar (hexagonal) phases. BMs were first discovered and studied in lyotropic sytems,[2] then in thermotropic (solvent-free) liquid crystals (LC)[3,4] and block and star polymers.[5–8] They can be used in photonics,[9,10] as 3D electronic or ionic conductors,[11,12] in membranes[13] and as templates for well-defined porous ceramics and metals for various uses.[14]

Classic lyotropic and block-polymer cubic BMs all contain two interpenetrating networks separated by a periodic surface of minimum curvature. They are of three types: double gyroid (DG, Figure 1a), double diamond (DD, Figure 1b) and double primitive (DP) or "Plumber's nightmare" (Figure 1c).[15,16] There are also equivalent structures with symmetry across the minimum surface broken, referred to as single network, although in block polymers they are more appropriately regarded as alternating network phases of 2 or sometimes 3 segregated microphases. These are nevertheless referred to as single gyroid (SG),[17] single diamond (SD)[18,19] and single primitive (SP)—Figures 1d–f. SG is also seen in some biological systems where the photonic effect of the chiral phase is responsible for structural color such as the intense colors of butterfly wings.[20,21] As true single networks it is perhaps more appropriate to think of structures that had used an alternating network and then converted one of them to ceramic or metal, while removing the other.[22]

In most thermotropic LC BMs the networks contain rod-like[3,4] or fan-like[23,24] aromatic cores lying perpendicular to the columnar network segments, displaying beside the achiral $Ia\bar{3}d$ gyroid[3,4] and a recent chiral $I4_132$ gyroid,[25] also a triple-network cubic $I23$[26] and a double-network tetragonal "Smectic-Q" ($I4_122$),[27] both chiral (not in Figure 1). In another type of thermotropic BMs the rods lie in bundles parallel to network segments, joined at junctions by flexible, usually hydrogen-bonded, links. Beside DG,[28,29] they have been found to form also DD,[30] SD,[31] SP,[32] as well as a SG alternating network phase.[33] It thus turns out that the classic jigsaw of BMs has been nearly completed by thermotropic LCs. However, one piece has been missing, in spite of several false claims in the past—the DP, the
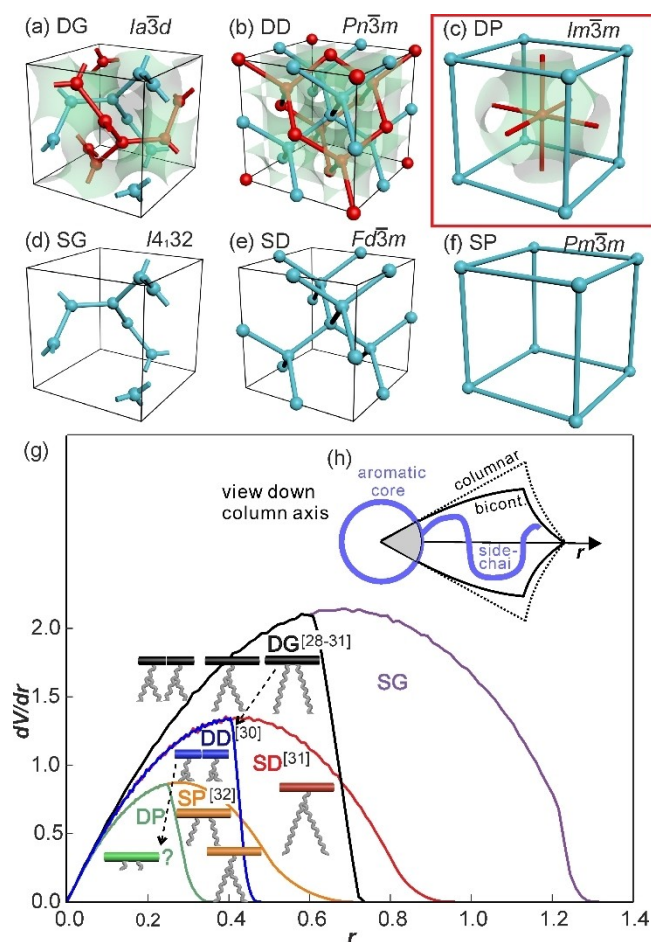
Figure 1. (a–c) Three double-network cubic phases with their infinite minimal surfaces (green) and (d–f) the corresponding single-network cubic phases, showing their abbreviations and space groups. (g) Radial distribution of volume functions dV/dr for the corresponding phases, where $V(r)$ is the fraction of the volume in the unit cell that is closest to a given network segment and at a distance r from it. The color-coded stylized molecules are actual published examples of glycerol-capped rod-like compounds with side-chains displaying bundle-type cubic mesophases of the corresponding type (references in brackets). Side-chain size is to scale with real molecules. The missing compound of unknown shape in DP is marked with "?". (h) A schematic view down a bundle (blue circle) with the time-averaged envelope of the side-chain(s) of one of its molecule.

"Plumber's nightmare", so prominent in lyotropics.[34] Here we explain why following previous design principles a thermotropic DP could not be realized and show how it can be obtained. The phase reported here is a LC structure of two tightly interwoven simple cubic networks consisting of stiff "struts" and flexible "hinges", and thus a true double framework. We also show how a subtle modification of molecular design changes the mesostructure completely, resulting instead in a complex array of countertwisting double helices.

A useful prop to understand the different geometries of BMs is presented in Figure 1g. It shows the rate of volume filling, dV/dr, with increasing radius of columnar network segments for the different BMs shown in Figure 1a–f. A

compound will adopt the phase whose dV/dr best matches the dynamically averaged shape of its molecules at a given temperature.[35] Using the example of bundle BMs, the circle in Figure 1h is a view along the bundle of rod-like molecular cores making up a network segment, while the wiggly blue line represents an attached side-chain contributing to the matrix continuum. For a columnar phase of parallel cylinders with no junctions the dV/dr would grow linearly until the cylinders clash, bringing dV/dr down to 0 when all space is filled. In cubic phases the junctions slow down the growth of dV/dr. For double network phases dV/dr drops abruptly when the two networks clash, whereas for single network phases it experiences soft landing as there is no second net to clash with. The curves in Figure 1g are all normalized to the same inter-junction distance. As can be seen, the double and single gyroid are the most loosely packed structures, requiring the largest side-chains to fill the inter-network space. Conversely, the SP and DP are the most tightly packed. The double-network versions are obviously packed twice as tightly, requiring the smallest side-groups. The schematic color-coded molecules are published examples of real compounds consisting of an aromatic glycerol-capped rigid rod with 1 or 2 linear or branched side-chains actually displaying the corresponding color-coded phase. The broken rods mean that two end-to-end molecules span the inter-junction distance. The size of the pendant chains in the sketches are to scale with that in the real molecules. Incidentally, while two alternating gyroids with $I4_132$ symmetry exist in thermotropics,[25,33] one with the second network missing altogether does not.

A thermotropic DP is however missing in any bicontinuous network-based incarnation, including any example of the expected $Im\overline{3}m$ spacegroup. According to Figure 1g its (green) molecules would need to have very short side-chains; follow the dashed arrows DG→DD→DP for easy comparison. However, a thermotropic LC compound needs two ingredients: an energy-lowering rigid core and an entropy-raising flexible component. Thus a molecule with very short chains, lacking the latter ingredient, would just crystallize. How to solve the problem and design a DP thermotropic? We decided to abandon the H-bonding glycerol core ends and move the flexible alkyl side-chains to the ends of the rods. Moreover, we incorporate a dithieno-fluorenone chromophore in the core to allow optical studies and prepare the ground for possible applications.

The target compound, abbreviated **FO-MeC16**, is shown in Table 1. Details of the synthesis and analytical data are given in Supporting Information. The material was studied by calorimetry (DSC) and powder small- and wide-angle X-ray scattering (SAXS/WAXS), grazing incidence SAXS (GISAXS) of surface-aligned thin films, by circular dichroism spectroscopy, second harmonic generation experiment, by electron density map construction and by simulation of diffraction pattern from structural models. The methods are described in SI.

The phase sequence and transition temperatures and enthalpies are listed in Table 1, and the DSC thermograms are shown in Figure S1 in SI. Polarized microscopy shows that the phase between the peaks at 38 and 60 °C on heating

Table 1: Chemical formula, molecular dimensions[a] and phase transition temperatures and enthalpies[b] of **FO-MeC16.**

Compound	a_{cub} (Å)	T [°C] (ΔH [J g^{-1}])
FO-MeC16	60.1	Cr 13 (15.1) Cub/$Im\overline{3}m$ 65(3.5) Iso

[a] L_{core} = length of aromatic core, L_{mol} = length of molecule with extended aliphatic chains. [b] Determined from DSC 2nd heating scan at 10 K min^{-1}. Cr = crystal, Cub/$Im\overline{3}m$ = cubic LC with $Im\overline{3}m$ symmetry, Iso = isotropic liquid.
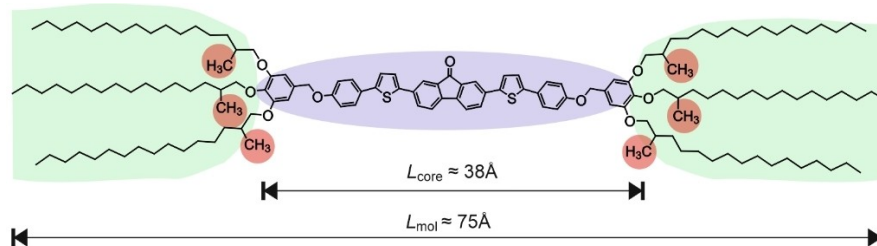
and between 58 and room temperature on cooling is optically isotropic, which suggests cubic symmetry. The WAXS pattern shows only a broad amorphous maximum at $q = 2\pi/4.5$ Å^{-1} (Figure 2a). This signals a lack of long-range order on the interatomic scale, confirming the LC nature of the phase. The Bragg reflections in the small-angle range have d^{-2} values in the ratio 1:2:3:4, and can thus be indexed as either (100), (200), (300), (400) of a primitive cubic lattice, or as (110), (200), (211), (220) of a body-centered cubic (Figure 2a). Grazing-incidence SAXS (GISAXS) experiment was performed on a surface-aligned sample to determine the Bravais lattice type. As shown in Figure 2b, the observed diffraction spots (left half) are consistent with

the (110), (200), (211), (220), *etc.* of a body-centered lattice; their calculated positions are shown on the right for a [110] axis perpendicular to the substrate. Five space groups fit the observed systematic absences, two of which are chiral. To test for chirality, circular dichroism (CD) spectra of a thin film were recorded as a function of temperature using a synchrotron-generated 50x50 µm^2 light beam that was small enough to avoid total cancellation of the signal in case of multiple small domains of random chirality. As shown in Figure S5, no CD was observed at any temperature in the LC range. As a result, two space groups were excluded, leaving only $Im\overline{3}$, $I\overline{4}3m$ and $Im\overline{3}m$. Next the material was examined for optical nonlinearity in a scanning optical microscope using an 800 nm laser. No second harmonic was generated, thus excluding the non-centrosymmetric $I\overline{4}3$ *m*.

Next electron density (ED) maps were constructed based on the two remaining spacegroup, using and different phase combinations. $Im\overline{3}m$ gave the most plausible USING measured intensities of the four observed Bragg reflections and their most plausible phase combination π0ππ resulted in the map in Figure 3a, where the blue and green domains represent, respectively, high and low ED, i.e. the aromatic and aliphatic regions. Identical maps were obtained for both $Im\overline{3}m$ and $Im\overline{3}$ spacegroups (Figure S4). This map strongly suggests a molecular model as in Figure 3b. The model agrees with the unit cell length of 60.1 Å (Table S1), being 15 Å shorter than the extended molecular length (75 Å), a shortfall attributed to coiling of the long alkyls. To further test the proposed structure, a geometric model of prisms and spheres of adjustable dimensions *w, l* and *r* (Figures S2–3) was constructed and its diffraction intensities calculated— for details see SI. The best-fit model is shown in Figure 3c and the good match between its calculated intensities and those observed is shown in Figure 2a. To illustrate the effect of the limited number of observed Bragg reflections, 4 in the present case, on resolution of the X-ray structure, the prism-sphere model in Figure 3c is represented by 4 Fourier terms, corresponding to the 4 observed Bragg reflections. The simulated map is shown in Figure 3d; this is how diffracted X-rays "see" the model in Figure 3c. It should be noted that the rounding of edges in Figures 3a,d results from genuine molecular motion in the LC. From the best-fit Debye–
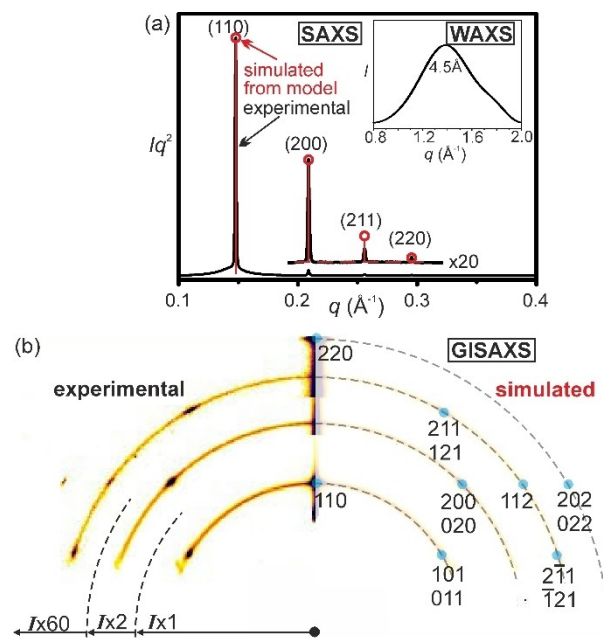

Figure 2. (a) Powder SAXS/WAXS pattern of **FO-MeC16** recorded in the cubic phase at 50°C; (b) experimental and simulated GISAXS pattern of **FO-MeC16** recorded at 50°C. The experimental GISAXS pattern is composed of three patterns on different intensity scales, as indicated. Simulated diffraction spots are shown on the right for (110) orientation of the body-centered cubic $Im\overline{3}m$.
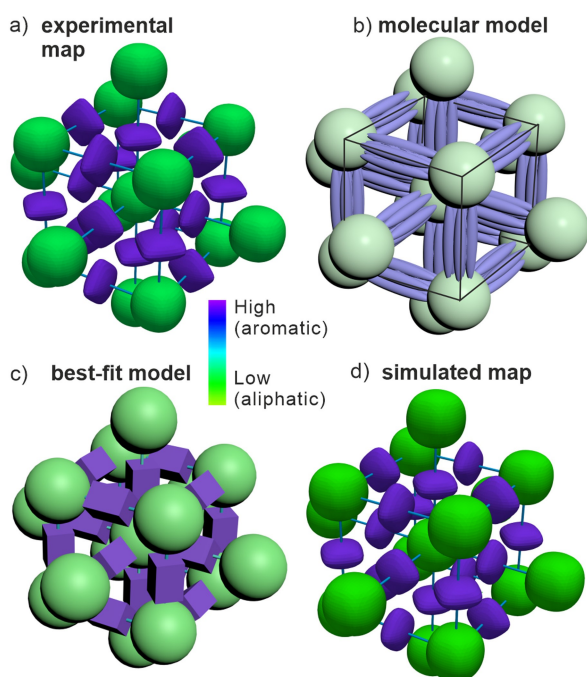
Figure 3. Electron density maps reconstructed from (a) experimental Bragg intensities and (d) best-fit model in (c). The model consists of (b) prisms and spheres representing bundles of rods and aggregated alkyl chains, respectively.

Figure 4. What a difference a methyl group makes: self-assembly of (a) **FO-C16** and (b) **FO-MeC16** into (c) helical columns or (d) coaxial bundles, respectively, resulting in fundamentally different LC phases—(e) a complex array of antichiral slow-twisting helices and (f) a cubic double framework of "struts" and "hinges". The latter is shown as it lies on its (110) face, as revealed by the GISAXS pattern in Figure 2b.

Waller factor used in the simulation, the mean-square displacement of an object (sphere or prism) is $\sqrt{\langle u^2 \rangle} = 16$ Å, which is as much as a quarter of the unit cell side (see SI, Sect. 3).

An additional proof that the derived structure is correct is the {110} orientation indicated by GISAXS. As shown in Figure 4f, by lying on a {110} plane the structure presents a smooth surface to the substrate with no need to break any molecular bundles as would be the case of {100} orientation shown in Figure 3. From the unit cell volume it is calculated (Table S2) that a bundle contains about 9 molecules, suggesting an average structure of 3 inner rods surrounded by 6 outer ones.

Thus the goal of achieving the first thermotropic double primitive (DP) "Plumber's nightmare" LC has been achieved, following the principles outlined in Figure 1. As usual, there was an element of good fortune in this feat. Rod-like molecules with 6 end-chains are long known to form columnar phases.[36] Indeed, as shown in Figure 4a,c,e, compound FO–C16, very similar to the current FO-MeC16 but lacking the methyl branch on the alkyls, displays a very different structure—a complex LC consisting of right- and left-twisted ribbons made up of stacked rafts of 2 side-by-side molecules lying normal to the column axis.[37] There are 8 double-helical columns running through an orthorhombic unit cell half a pitch in height, spacegroup *Fddd*.[37,38,39] One may ask why a small methyl group should make such a drastic difference to the packing mode. We propose that the key is in the position of the group, i.e. very close to the aromatic-aliphatic interface. This aggravates the cross-sec-
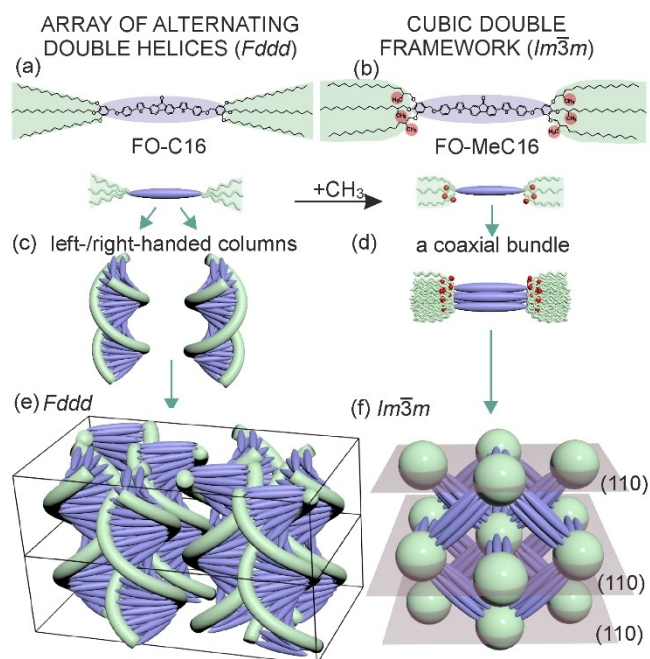
tional mismatch and the overcrowding at the interface. While the gradual taper of the FO–C16 (Figure 4a) fits the *dV/dr* curve for a columnar phase (Figure 1h), the abrupt widening at the critical interface in FO-MeC16 does not (Figure 4b). Had the branch been placed further away along the chain, a columnar-type phase would have prevailed, as some of our preliminary experiments suggest. As it is, the FO-MeC16 had no choice but to adopt an alternative new LC structure. This result for the first time makes a connection between the two types of self-assembly of rod-like molecules: those with multiple end-chains lying transverse to the column in columnar and cubic phases, and those with side-chains forming bundle-type phases with coaxial molecules.

This work has shown, as often before, that incorporation of a strategically placed disrupting element, in this case a proximate methyl group, is an effective way to generate new modes of self-assembly. The current DP is the second known type of liquid organic framework, the first, formed by side-chain bolaamphiphiles, being of the looser SP type.[32] Unlike the SP, which can be regarded as analogous to crystalline MOFs and COFs, here the voids are filled with the second network. This LC phase is unique in that there is only one continuous subphase with direct lateral contact between π-conjugated mesogenic moieties, potentially enabling electron or hole passage uninterrupted by another continuous sub-phase; the interruptions are confined to isolated aliphatic islands. The phase can be considered as an inverse of the body-centered micellar LC found mainly in

Angew. Chem. Int. Ed. **2024**, e202413215 (4 of 5)

© 2024 The Authors. Angewandte Chemie International Edition published by Wiley-VCH GmbH

dendrons.[40,41] Further studies continue, exploring the effects of chain length, their branching, and chirality.

Conflict of Interest

The authors declare no conflict of interest.

Data Availability Statement

The data that support the findings of this study are available in the supplementary material of this article.

[1] G. Ungar, X. B. Zeng, *Soft Matter* **2005**, *1*, 95–106.

[2] V. Luzzati, T. Gulik-Krzywicki, A. Tardieu, *Nature* **1968**, *218*, 1031–1034.

[3] J. Malthête, A. M. Levelut, N. H. Tinh, *J. Physique Lett.* **1985**, *46*, 875–880.

[4] M. Clerc, E. Dubois-Violette, *J. de Physique II.* **1994**, *4*, 275–286.

[5] E. L. Thomas, D. M. Anderson, C. S. Henkee, D. Hoffmann, *Nature* **1988**, *334*, 598–601.

[6] J. Chatterjee, S. Jain, F. S. Bates, *Macromolecules* **2007**, *40*, 2882–2896.

[7] J. J. K. Kirkensgaard, M. E. Evans, L. D. Campo, S. T. Hyde, *Proc. Nat. Acad. Sci.* **2014**, *111*, 1271–1276.

[8] H. Lee, S. Kwon, J. Min, S. M. Jin, J. H. Hwang, E. Lee, W. B. Lee, M. J. Park, *Science* **2024**, *383*(6678), 70–76.

[9] M. Maldovan, A. M. Urbas, N. Yufa, W. C. Carter, E. L. Thomas, *Phys. Rev. B.* **2002**, *65*, 165123.

[10] M. Saba, B. D. Wilts, J. Hielscher, G. E. Schroeder-Turk, *Mater. Today: Proc.* **2014**, *1*, 193–208.

[11] J. L. Blin, M. Impéror-Clerc, *Chem. Soc. Rev.* **2013**, *42*, 4071–4082.

[12] T. Kato, M. Yoshio, T. Ichikawa, B. Soberats, H. Ohno, M. Funahashi, *Nat. Rev. Mater.* **2017**, *2*, 17001.

[13] T. Kato, J. Uchida, Y. Ishii, G. Watanabe, *Adv. Sci.* **2023**, 202306529.

[14] R. P. Thedford, P. A. Beaucage, E. M. Susca, C. A. Chao, K. C. Nowack, R. B. Van Dover, S. M. Gruner, U. Wiesner, *Adv. Funct. Mater.* **2021**, *31*, 202100469.

[15] V. Luzzati, R. Vargas, P. Mariani, A. Gulik, H. Delacroix, *J. Mol. Biol.* **1993**, *229*, 540–551.

[16] G. Lindblom, L. Ralfors, *Biochlm. Blophys. Acta* **1989**, *988*, 221–256.

[17] M. Seki, J. Suzuki, Y. Matsushita, *J. Appl. Crystallogr.* **2000**, *33*, 285–290.

[18] D. Abdelrahman et al, *ACS Appl. Mater. Interfaces* **2023**, *15*, 57981–57991.

[19] D. Moschovas, et al., *Nanomaterials* **2020**, *10*, 1497.

[20] V. Saranathan, C. O. Osuji, S. G. J. Mochrie, H. Noh, S. Narayanan, A. Sandy, E. R. Dufresne, R. O. Prum, *Proc. Natl. Acad. Sci. USA* **2010**, *107*, 11676–11681.

[21] K. Michielsen, H. De Raedt, D. G. Stavenga, *J. R. Soc. Interface* **2010**, *7*, 765–771.

[22] L. Wu, W. Zhang, D. Zhang, *Small* **2015**, *11*, 5004–5022.

[23] S. N. Chvalun, M. A. Shcherbina, A. N. Yakunin, J. Black-well J, V. Percec, *Polymer Sci. Ser A.* **2007**, *49*, 158–167.

[24] T. Ichikawa, M. Yoshio, A. Hamasaki, S. Taguchi, F. Liu, X. B. Zeng, G. Ungar, H. Ohno, T. Kato, *J. Am. Chem. Soc.* **2012**, *134*, 2634–2643.

[25] Y. Wang, S.-G. Yang, Y.-X. Li, Y. Cao, F. Liu, X.-B. Zeng, L. Cseh, G. Ungar, *Angew. Chem. Int. Ed.* **2024**, *63*, e202403156.

[26] X. B. Zeng, G. Ungar, *J. Mater. Chem. C* **2020**, *8*, 5389–5398.

[27] H. J. Lu, X. B. Zeng, G. Ungar, C. Dressel, C. Tschierske, *Angew. Chem. Int. Ed.* **2018**, *57*, 2835–2840.

[28] F. Liu, M. Prehm, X. B. Zeng, C. Tschierske, G. Ungar, *J. Am. Chem. Soc.* **2014**, *136*, 6846–6849.

[29] S. Poppe, C. L. Chen, F. Liu, C. Tschierske, *Chem. Commun.* **2018**, *54*, 11196–11199.

[30] X. B. Zeng, M. Prehm, G. Ungar, C. Tschierske, F. Liu, *Angew. Chem. Int. Ed.* **2016**, *55*, 8324–8327.

[31] X. B. Zeng, S. Poppe, A. Lehmann, M. Prehm, C. L. Chen, F. Liu, H. J. Lu, G. Ungar, C. Tschierske, *Angew. Chem. Int. Ed.* **2019**, *58*, 7375–7379.

[32] S. Poppe, X. Cheng, C. Chen, X. B. Zeng, F. Liu, G. Ungar, C. Tschierske, *J. Am. Chem. Soc.* **2020**, *142*, 3296–3300.

[33] C. L. Chen, R. Kieffer, H. Ebert, M. Prehm, R. B. Zhang, X. B. Zeng, F. Liu, G. Ungar, C. Tschierske, *Angew. Chem. Int. Ed.* **2020**, *59*, 2725–2729.

[34] Unfortunately the DP phase is now routinely referred to as "primitive" in the lyotropic community, although its Bravais lattice is decidedly not primitive but body centered.

[35] X. B. Zeng, G. Ungar, M. Impéror-Clerc, *Nat. Mater.* **2005**, *4*, 562–567.

[36] J. Malthête, A. M. Levelut, N. H. Tinh, *J. Phys. Lett.* **1985**, *46*, L875–L880.

[37] Y. X. Li, H. F. Gao, R. B. Zhang, K. Gabana, Q. Chang, G. A. Gehring, X. H. Cheng, X. B. Zeng, G. Ungar, *Nature Commun* **2022**, *13*, 384.

[38] P. Rybak, A. Krowczynski, J. Szydlowska, D. Pociecha, E. Gorecka, *Soft Matter* **2022**, *18*, 2006–2011.

[39] Y. Wang, Y. X. Li, L. Cseh, Y. X. Chen, S. G. Yang, X. B. Zeng, R. B. Zhang, F. Liu, W. B. Hu, G. Ungar, *J. Am. Chem. Soc.* **2023**, *145*, 17443–17460.

[40] D. J. P. Yeardley, G. Ungar, V. Percec, N. M. Holerca, G. Johansson, *J. Am. Chem. Soc.* **2000**, *122*, 1684–1689.

[41] X. H. Yao, L. Cseh, X. B. Zeng, M. Xue, Y. S. Liu, G. Ungar, *Nanoscale Horiz.* **2017**, *2*, 43–49.

Communication

Y.-X. Li, R.-Y. Jia, G. Ungar,* T. Ma, K. Zhao,
X.-B. Zeng,* X.-H. Cheng* — **e202413215**

Thermotropic "Plumber's Nightmare"—A
Tight Liquid Organic Double Framework
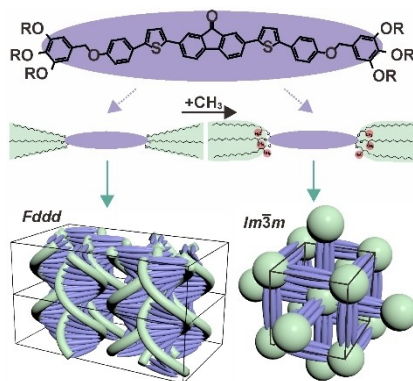
A most common cubic phase in lyotropic (surfactant-water) systems, the "plumber's nightmare" labyrinth, has never been found in thermotropic liquid crystals. Here the first example is reported. Intriguingly, removal of just a methyl branch from the fluorescent mesogen's six alkyls converts the double-network cubic into an array of counter-twisting helices.